2013 International Conference on Unmanned Aircraft Systems (ICUAS)
May 28-31, 2013, Grand Hyatt Atlanta, Atlanta, GA

A Hyper-Redundant Manipulator for Mobile Manipulating Unmanned Aerial Vehicles

Todd W. Danko[1] and Paul Y. Oh[1]

Abstract— **Due to their ability to navigate in 6 degree of freedom space, Unmanned Aerial Vehicles (UAVs) can access many locations that are inaccessible to ground vehicles. While mobile manipulation is an extremely active field of research for ground traveling host platforms, UAVs have historically been used for applications that avoid interaction with their environment at all costs. Recent efforts have been aimed at equipping UAVs with dexterous manipulators in an attempt to allow these Mobile Manipulating UAVs (MM-UAVs) to perform meaningful tasks such as infrastructure repair, disaster response, casualty extraction, and cargo resupply.**

Among many challenges associated with the successful manipulation of objects from a UAV host platform include: a) the manipulator's movements and interaction with objects negatively impact the host platform's stability and b) movements of the host platform, even when using highly accurate motion capture systems for position control, translate to poor end effector position control relative to fixed objects.

To address these two problems, we propose the use of a hyper-redundant manipulator for MM-UAV applications. The benefits of such a manipulator are that it: a) can be controlled in such a way that links are moved within the arm's free space to help reduce negative impacts on the host platform's stability and b) the redundancy of the arm affords a highly reachable workspace for the end effector, allowing the end effector to track environmental objects smoothly despite host platform motions.

This paper describes the design of a hyper-redundant manipulator suitable for studying its applicability to MM-UAV applications and provides preliminary results from its initial testing while mounted on a stationary scaffold.

I. Introduction

Unmanned Aerial Vehicles (UAVs), originally deployed as target drones for combat pilot training have evolved over time to provide valuable roles in Intelligence, Surveillance and Reconnaissance for both civilian and military operations. Historically, UAVs have been built and operated in ways to avoid interacting with their environment at all costs, affording them the ability to quickly and efficiently travel large distances, while minimizing path planning complexity. The ability for aerial vehicles to manipulate or carry objects that they encounter could greatly expand the types of missions achievable by unmanned aerial systems. High degree of freedom robots with dexterous arms could lead to transformative applications in near-Earth, outer space, and underwater environments.

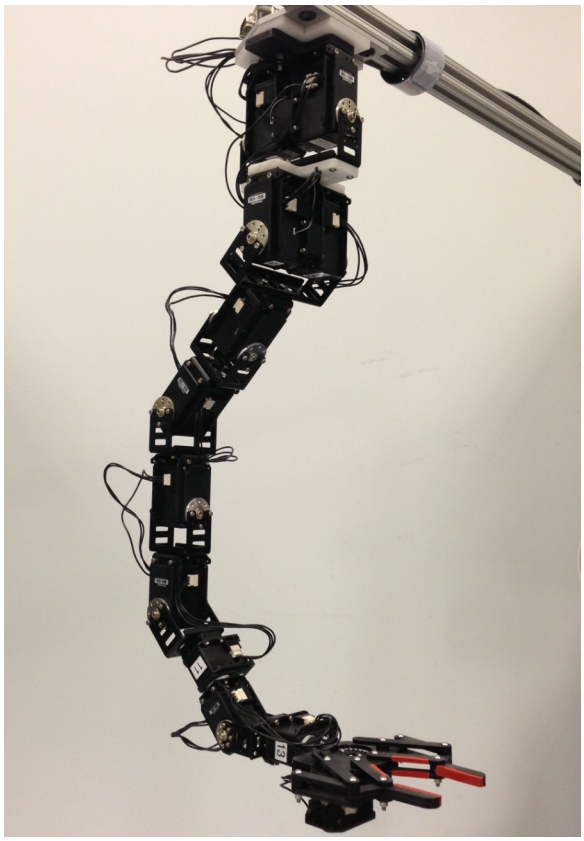

Fig. 1. Hyper-redundant manipulator designed for MM-UAV

This project was supported in part by a US NSF CRI II-New, Award # CNS-1205490

[1]Drexel Autonomous Systems Lab, Drexel University, Philadelphia, PA, USA todd.danko@drexel.edu, paul@coe.drexel.edu

Such applications could include infrastructure repair, disaster response, casualty extraction, and cargo resupply, leading to a paradigm shift in the way UAVs are deployed.

While mobile manipulation continues to be a highly active field of study, much of the focus lies with ground vehicles that provide a passively stable base during manipulation. Some researchers have achieved aerial grasping through the use of 1 degree of freedom grippers [1], [2]. While these results are valuable, they implement simple grasping rather than true manipulation. The host platform provides the extent of the manipulation degrees of freedom. MM-UAV efforts are inspired by nature, to implement true dexterous manipulation from aerial vehicles in ways that are similar to how an octopus can use its tentacles to manipulate objects like seashells while walking on the ocean floor or swimming with its remaining tentacles.

Towards realizing our vision of MM-UAV, we explore the use of a hyper-redundant tentacle-like manipulator as shown in Figure 1 that has the following advantages:

1) Highly redundant manipulators have large reachable spaces, affording reliable access to end effector poses while reducing the requirements on platform positioning accuracy.
2) The hyper-redundant manipulator itself can be used as an end effector to interact with certain types of objects that are not necessarily graspable with the installed end effector.
3) A high degree of redundancy allows for a controller to take advantage of link motions in the manipulator's free space, which can be used to either impact or minimize arm's influence on the host platform's dynamic state as desired.

Our goal in constructing this hyper-redundant manipulator is not necessarily to fly this specific model on a UAV, but to allow us to study the fundamentally open research issues of reaction forces and torques associated with MM-UAVs interacting with their environment. Despite this primary goal, it is be possible to mount a manipulator by this design onto larger scale UAVs such as the Rotomotion SR 20 robotic helicopter. Additionally, the lessons learned from this effort may be leveraged in the future to construct a smaller, lighter version for use with quad-rotors such as the Ascending Technologies Pelican.

II. Related Work

Highly dexterous manipulators on ground-based systems are of great interest for commercial and military applications due to their ability to interact with their environment. NASA's Robonaut, University of Massachusetts' uBot, Willow Garage's PR2, and CMU's HERB all include dual manipulators fixed to a mobile base. There are also many fixed base dual arm systems such as DARPA's ARM Robot, Massachusetts Institute of Technology's DOMO, and University of Massachusetts' Dexter robot. The systems most related to our design include those on a mobile base that must dynamically balance during the manipulation task. In particular, we believe there are significant similarities between MM-UAV and humanoids. The Humanoid PIRE (Partnership for International Research and Education) hosted by Drexel University and funded through the National Science Foundation is using full-scale, mini, and virtual HUBO platforms to study bipedal locomotion and grasping [10]. Humanoids such as HUBO and the DARPA Robotics Challenge Atlas robot share our challenge of compensating for a constantly changing center of gravity during whole body locomotion and manipulation.

In addition to leveraging work on manipulators attached to ground vehicles and humanoids, we will take advantage of advances in UAV technologies. Autonomy for rotary-wing unmanned air vehicles is being studied at numerous universities, research centers, and private companies, which will help stabilize our platform. Advances in materials and electronics have allowed researchers to achieve small form-factors and light weights [3], [4]. There are a number of aerial testbeds to study single and multi-robot coordination and perform algorithm testing [5], [6]. Many laboratories use motion capture systems, implementing an array of high-speed cameras in an indoor chamber. With improvements in mobile manipulation techniques, particularly with ground robots, these methods are now being applied to aerial vehicles as well [14]. The Yale Aerial Manipulator can grasp and transport objects using a compliant gripper attached

TABLE I
DENAVIT-HARTENBERG PARAMETERS FOR THE HYPER-REDUNDANT MANIPULATOR

Link Number	θ (rad.)	d (mm)	a (mm)	α (rad.)
1	0	0	96.8	$-\pi/2$
2	0	0	90.5	$\pi/2$
3	0	0	90.5	$-\pi/2$
4	0	0	88	$\pi/2$
5	0	0	88	$-\pi/2$
6	0	0	77.8	$\pi/2$
7	0	0	71.8	$-\pi/2$
8	0	0	0	$-3\pi/2$
9	0	190.2	0	$-\pi/2$

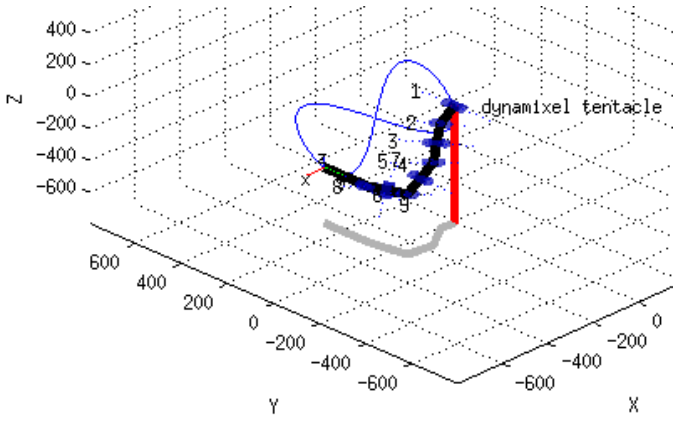

Fig. 2. Model of the hyper-redundant manipulator sweeping through a figure "8" test pattern

to the bottom of a T-Rex 600 RC helicopter [7]. Researchers at the GRASP Lab at the University of Pennsylvania are using multiple quadrotors to transport payloads in three dimensions using cables or a gripper [8]. Previous research at Drexel has produced a prototype UAV pickup mechanism with a hook to deliver and retrieve cargo [9]. While there are numerous ground vehicles that use highly dexterous arms, very few if any small or even large UAVs have multiple degree of freedom manipulators mounted to them. To draw a comparison with biology, most UAV manipulators imitate a bird with a beak or claw opening and closing in a 1 degree of freedom movement. Our goal is ultimately to integrate a bulbous head with multiple arms similar to an octopus. We aim to leverage the state of the art in ground-based mobile manipulators and apply that to aerial vehicles.

III. HYPER-REDUNDANT MANIPULATOR

A. Arm Description

The hyper-redundant arm is assembled from off the shelf Dynamixel servo motors and brackets as shown in Figure 1. The Denavit-Hartenberg parameters that represent the nine joints of this arm are listed in Table I. This model is used in Matlab [11] as shown in Figure 2 to rapidly develop and test motion controllers without an initial need for a motion capture system and accurate torque sensors at each joint to measure ground truth.

B. Hand Description

The hand is a custom designed gripper with two degrees of freedom and 1 degree of control. A single Dynamixel servo motor controls the opening and closing of the fingers, while a spring mechanism allows the fingers to passively conform around convex objects. This is accomplished by allowing the finger tips to close inward after the knuckle joints have collided with the grasped object. A mechanical stop prevents the fingers from opening wider than a parallel jaw configuration making the hand suitable for performing pinch grasps as shown in Figure 3.

C. Position Control

Inverse kinematics calculations are used to identify positions for each joint of the manipulator (q) that when executed, result in the end effector reaching a desired position and orientation. Redundat manipulators, manipulators that have a greater number of degrees of actuation than degrees of freedom, can generally achieve a desired end effector position though a very large number of unique joint configurations, making the identification of a desirable joint space solution elusive. Multiple approaches have been explored for calculating the inverse kinematics for this hyper-redundant manipulator including a pseudo-inverse Jacobian, weighted pseudo-inverse Jacobian and finally a heuristic approach.

1) Pseudo-Inverse Jacobian Inverse Kinematics: The pseudo-inverse Jacobian is an iterative

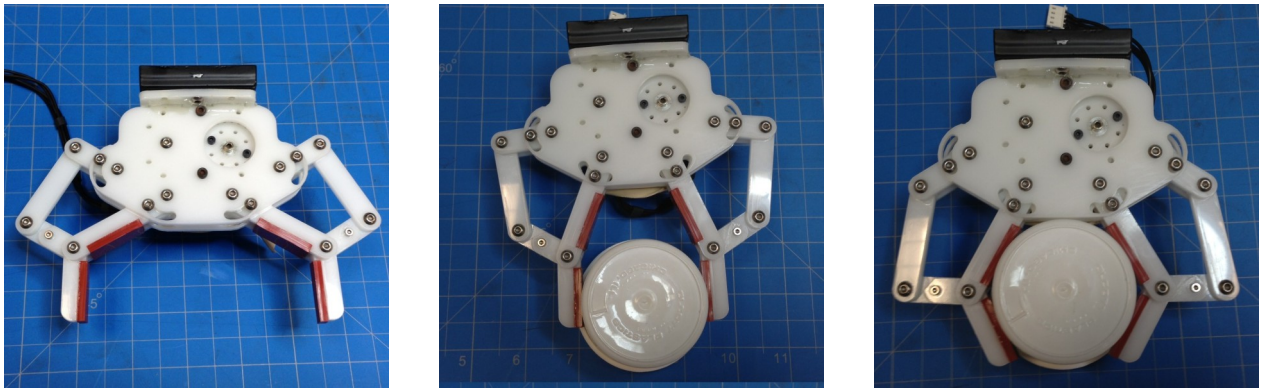

(a) Jaws Open (b) Pinching Grasp (c) Passively Compliant Caging Grasp

Fig. 3. Passively compliant 2 degree of freedom gripper with 1 degree of actuation allows the hyper-redundant arm to grasp a wide variety of objects with minimal grasp planning

approach that seeks to minimize the error between the desired and current end effector positions, ultimately solving q which represents the resulting joint positions for the manipulator.

$$q = q_{previous} + \alpha \times \dot{q} \tag{1}$$

Where α starts at a value of 1 and is decreased if the solution begins to diverge during iteration and:

$$\dot{q} = J^{\#} \times [X_0 - X] \tag{2}$$

Where $[X_0 - X]$ is the 6 degree of freedom error between the desired and current end effector positions and $J^{\#}$ is the pseudo inverse of the manipulator's Jacobian J:

$$J^{\#} = J^T \times (J \times J^T)^{-1} \tag{3}$$

2) Weighted Pseudo-Inverse Jacobian Inverse Kinematics: The weighted pseudo-inverse Jacobian is similar to the pseudo-inverse Jacobian except that $\dot{q}$ is calculated:

$$\dot{q} = W^{-1} J^{\#T} (J^{\#} W^{-1} J^{\#T})^{-1} [X_0 - X] \tag{4}$$

Where:

$$W = K_w |(|q + \dot{q}| - |q_{previous}|)| \tag{5}$$

K_w is a weighting gain that must be adjusted to tune the algorithm to sufficiently avoid solutions where joints are commanded to positions close to their limits. For our hyper-redundant manipulator, we achieved satisfactory results by setting $K_w = 1000$. It should be noted that q and $\dot{q}$ in 5 must be pre-calculated using the standard pseudo-inverse Jacobian approach described in 1 and 2. Small weighting values for a joint in W results in the joint being used to a greater extent to reach the end effector target, while large values reduce the use of a given joint.

3) Heuristic Inverse Kinematics: Finally, we considered a heuristic inverse kinematics algorithm that is as described in [12]. This heuristic algorithm calculates joint angles to achieve a desired end effector pose as follows:

1) Use forward kinematics to calculate the distance between the end effector and the gaol position.
2) Calculate the impact on end effector closeness to the goal as each joint is independently moved up and down from its original position by an angle ($\Delta\theta$) without exceeding specified joint limits. An initial value of $\Delta\theta = \pi/4$.
3) Analyze the results of step 2, selecting the joint and direction that resulted in the smallest subsequent end effector to goal difference.
4) Apply the joint position identified in step 3 if it produces a smaller error that what was identified in step 1 and return to step 1, otherwise divide $\Delta\theta$ in half and return to step 2.
5) End when the end effector is closer than a desired threshold to the goal position.

TABLE II

IK PERFORMANCE WHILE FOLLOWING A FIGURE "8" PATTERN AND REACHING RANDOM LOCATIONS AND ORIENTATIONS

Algorithm	Pattern	Time	Random	Time
Pseudo-Inverse Jacobian	96.6%	0.047s	48.0%	0.192s
Weighted Pseudo-Inverse Jacobian	99.8%	0.089s	82.6%	0.465s
Heuristic	100.0%	2.121s	84.1%	3.031s

D. Reachability Evaluation

The inverse kinematics solvers are evaluated for our application though analysis of the arm's reachability while using each algorithm in various scenarios. The first test scenario involves solving for joint angles so that the end effector reaches a series of randomly generated, but known reachable points in space. The points are known to be reachable because they are derived using forward kinematics from randomly generated, valid angles for each joint in the arm. The ratio of successes to attempts for reaching these points with the hyper-redundant arm serves as a reachability metric. Reachability metrics for each of the previously described inverse kinematics algorithms are documented in Table II, where success is measured as the end effector achieving a position that is within 1mm of the goal position without violating joint angle limits.

While it is useful to be able to command a robotic arm to arbitrary positions, fluid motion trajectories are often represented as a series of either position or velocity waypoints. To test reachability against this scenario, we present a figure "8" pattern to each inverse kinematics solver that is being evaluated. This figure "8" pattern has been broken up into 1000 waypoints. Reliability of tracking this pattern is also presented in Table II, where the percentage of 1000 test points that are within 1mm of the goal, and do not violate joint constraints are shown along with the average convergence time for good solutions.

The times shown in Table II were all calculated on the same computer with the inverse kinematics function being the only variable. While these times will be longer or shorter on other computers, they serve as a relative comparison between the time it takes to calculate joint angles for the various scenarios. It is expected that the randomly accessed end effector poses will always take longer to converge on a solution than for following a pattern. This is because for pattern following, the previous end effector position is very close to the current position being calculated, so the previous joint angles serve as a close starting point for the current calculation. The random end effector positions are always calculated from a default ready position that is not necessarily near the current end effector position of interest. It can be seen that the inverse Jacobian algorithm is the fastest for both pattern following and accessing random points in space, but it can also be seen that it provides the worst performance in actually reaching desired end effector poses. The heuristic approach is most reliable at reaching positions, but is by far the slowest, taking seconds to converge on solutions making it unable to keep up the with dynamic positioning requirements of MM-UAV. The weighted inverse Jacobian algorithm is reasonably fast, and is more reliable than the inverse Jacobian algorithm.

The inverse Jacobian algorithm does not consider joint angle limits while calculating joint positions, while the weighted inverse Jacobian de-weights joints that are moving towards their limits. This limit based joint de-weighting does not guarantee that joints will be commanded to valid ranges between set limits, but it makes it more common as shown by the improvement in successfully converging on solutions. The heuristic algorithm is guaranteed to return only valid joint angles.

E. Force Control

Even with excellent vehicle and object position information provided by motion capture systems, relative motions between the UAV and the object to manipulate provide challenges that position only controllers are poorly equipped to handle. Attempts to perform manipulations from an aerial vehicle without a motion capture system exacerbate these uncertainties, highlighting the need for compliant manipulation approaches. Hardware compliance has been employed in [1], but to address the difficulties of using rigid, redundant manipulators, force control must be explored. Applying a portion of the work presented in [13], we have modified our controller to at times apply

prescribed interaction forces at the end effector which are calculated as follows:

$$F_{int} = K[X_0 - X] \tag{6}$$

Where F_{int} is the desired interaction force to be applied at the end effector, and $X_0 - X$ is the position error and K is a stiffness gain to map between position error and interaction force. K can be thought of as a spring constant while $X_0 - X$ can be thought of as the spring's compression. 6 can be rearranged to solve for a pseudo-goal position to command the end effector to, using the position controller that will impart the desired amount of force. To achieve this, we need to calculate the torques necessary to command to each joint T_{act}:

$$T_{act} = J^{\#T} F_{int} \tag{7}$$

Combining 6 and 7, we have:

$$T_{act} = J^{\#T} K[X_0 - X] \tag{8}$$

An example of the use of hybrid position-force control can be seen in Figure 4, where the hyper-redundant manipulator has been commanded to wrap compliantly around an object in the environment. Commanding torques to each servo motor allows for each link to press against the environmental feature, allowing the feature to guide the hyper-redundant manipulator's pose just as much as the position controller does. The availability of 9 degrees of freedom makes it possible for the arm to be used in such a way for prehensile grasps, which is something that 6 and 7 degree of freedom manipulators can not do, even when taking advantage of the additional degrees of freedom afforded by the host platform. Such manipulations can augment the types of objects that are graspable to the system to include a broader set of graspable features, and also, when combined with multiple manipulators, may eventually provide the ability to perch in complex environments while performing other manipulations.

IV. Preliminary Demonstration

A preliminary demonstration of the hyper-redundant manipulator's capabilities was performed by picking up a block from a peg, then stacking it onto a neighboring peg. Screen captures from this demonstration can be seen in Figure 5. To prepare the hyper-redundant manipulator to perform this block transfer task, the location of the tops of the source and destination pegs were established in the manipulator's coordinate system through manual measurement. The height of the pegs were also measured. A series of waypoints were automatically calculated that serve to move the arm through the various stages of the manipulation:

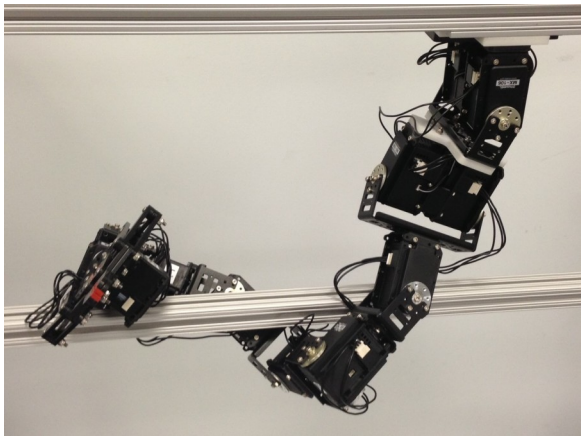

Fig. 4. Hyper-redundant manipulator being used to interact with an object rather than serving to only position the end effector

1) The manipulator starts in a ready position as shown in Figure 5a.
2) The first waypoint to move to is 2cm above the source peg as shown in Figure 5b. The reason for moving to a position above the peg rather than directly to the block at the peg's base is to ensure that no part of the manipulator collides with the peg during its approach.
3) The gripper is commanded to open its fingers as wide as possible to achieve a pre-grasp configuration.
4) The second waypoint brings the end effector down to the base of the source peg as shown in Figure 5c where the gripper is commanded to close around the block with a pre-defined closing force that achieves a balance between grasp strength and potential servo damage.
5) The third waypoint is identical to the first waypoint, and upon execution, lifts the block up and off of the source peg as shown in 5d.

6) The fourth waypoint is 2cm above the destination peg as shown in Figures 5e and 5f.
7) Due to limitations in the repeatability of the hyper-redundant manipulator, the block is not well enough aligned with the destination peg to simply slide the block down over the peg. Rather than attempting to force the block down to the base of the peg, a waypoint is specified that is 5mm below the top of the peg, and the end effector is commanded to attempt to reach this waypoint using a hyprid position-force control approach, therefor applying a mating pressure in the z direction. The end effector position is then dithered in the x and y positions over a radius of 1.5cm. The dither process is continued until it is detected that the end effector has reached the waypoint that is 5mm below the top of the destination peg, indicating that the peg has slid into the hole.
8) Once the block has been mated to the destination peg, the end effector proceeds to a waypoint that is at the base of the destination peg as shown in 5g.
9) With the block placed in its desired position, the gripper is opened, releasing the block, and then the end effector moves to a waypoint above the destination peg, and finally returns to the manipulator's ready position as shown in Figure 5h.

V. Conclusion And Future Work

A. Conclusion

We have described our initial design and experimentation with a hyper-redundant manipulator as applied to the MM-UAV problem. Our ultimate goal is to create a fully functioning flying prototype that makes use of multiple similar hyper-redundant manipulators to perform a wide variety of autonomous tasks, mimicking and extending the work performed with autonomous and teleoperated manipulators mounted to ground vehicles. In this paper, we discussed multiple inverse kinematics solvers, and have identified the weighted pseudo-inverse Jacobian method to be the best fit for our MM-UAV hyper-redundant manipulator because of its ability to reliably and quickly achieve desired poses.

B. Future Work

The research performed to date on the use of a hyper-redundant manipulator for MM-UAV has led to certain lessons learned, and inspired multiple follow-on studies including:

1) The current hyper-redundant manipulator does not include a spherical wrist. Through preliminary reachability analysis, it has been shown that the addition of a spherical wrist to this hyper-redundant manipulator improves the reachable arm volume, for our specific design, by over 20%, so a design to include a spherical wrist will be considered.
2) Closed-form inverse kinematics solutions may be used to directly calculate joint positions from desired end effector poses. This is complicated for a hyper-redundant manipulator because for our 9 degree of freedom manipulator, there are 84 potential combinations of six joints, with three free joints. While this number of combinations is tractable to calculate, assuming that the arm is modified to include spherical wrist joints, they must always be used, leaving only 20 possible combinations for free joints. Further the two shoulder joints have the greatest impact on the volume of the arm's reachable work space, so removing these from consideration for free joints along with the spherical wrist leaves a total of four sets of possible free joints, making closed-form inverse kinematic solutions straight forward.
3) Using a closed-form inverse kinematics solver, the free joints may be moved without impacting the end effector's position. Free joint motions must be explored as a way to beneficially offset overall manipulator motions and interaction forces as they influence host platform stability.
4) The current hyper-redundant arm is mounted to a rigid scaffold which is useful for the early evaluation of motion control, however to provide true relevance to the MM-UAV problem, the arm must be mounted to a movable gantry that can be both actively driven to simulate motions from the host UAV, and also passively moved by motions and interaction forces from the manipulator.

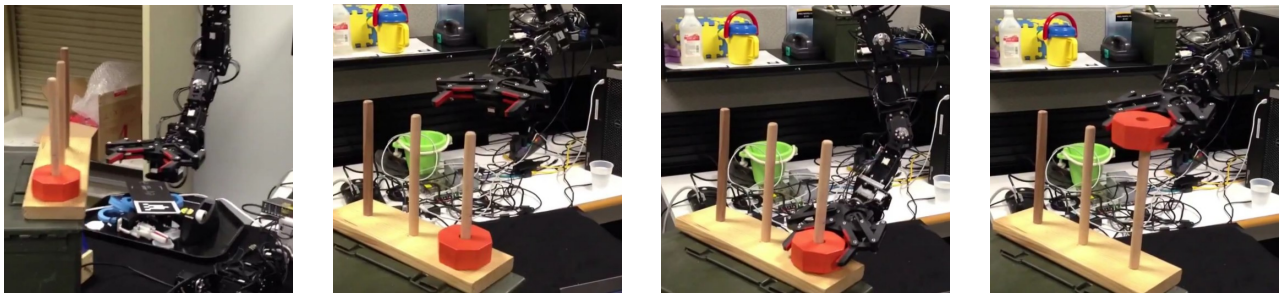

(a) Ready Position (b) Approach (c) Grasp Block (d) Lift Block Off Post

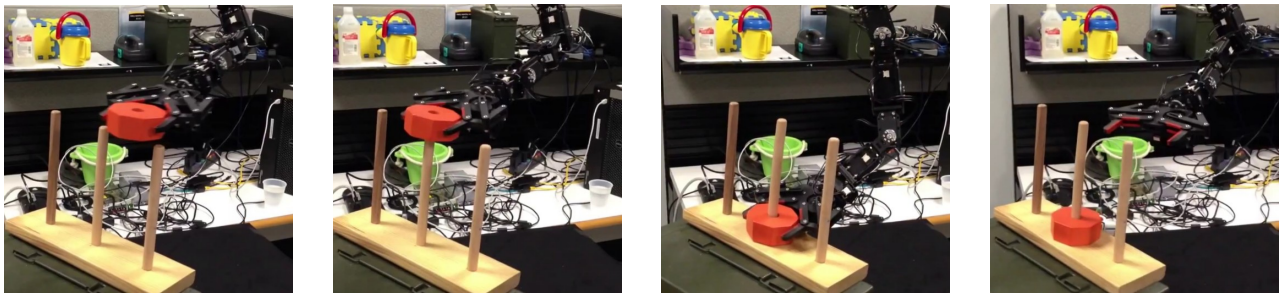

(e) Move Block Between Posts (f) Align Block to Post (g) Slide Block Down Post (h) Return to Ready Position

Fig. 5. Video frames from a block transfer demonstration (http://youtu.be/oDHmaUrWGww)

5) Ultimately our goal is to fly a hyper-redundant manipulator such as this on either a larger scale UAV such as the Rotomotion SR 20 robotic helicopter or to scale our design both in size and weight to be mounted on a smaller platform such as the Ascending Technologies Pelican.

REFERENCES

[1] P. E. I. Pounds, D. R. Bersak and A. M. Dollar, "Grasping from the air: Hovering capture and load stability," in IEEE Int Robotics and Automation (ICRA) Conf, 2011.

[2] D. Mellinger, Q. Lindsey, M. Shomin and V. Kumar, "Design, modeling, estimation and control for aerial grasping and manipulation," in IEEE/RSJ Int Intelligent Robots and Systems (IROS) Conf, 2011.

[3] D. Pines and F. Bohorquez, Challenges facing future micro air vehicle development, AIAA Journal of Aircraft, vol. 43, no. 2, pp. 290305, 2006.

[4] B. Hein and I. Chopra, Hover performance of a micro air vehicle: Rotor at low reynolds number, Journal of the American Helicopter Society, vol. 52, no. 3, pp. 254262, July 2007.

[5] N. Michael, D. Mellinger, Q. Lindsey, and V. Kumar, The GRASP Multiple Micro UAV Testbed, in IEEE Robotics and Automation Magazine, Sept. 2010.

[6] G. Hoffmann, D. Rajnarayan, S. Waslander, D. Dostal, J. Jang, and C. Tomlin, The Stanford Testbed of Autonomous Rotorcraft for Multi-Agent Control, in the Digital Avionics System Conference 2004, Salt Lake City, UT, November 2004.

[7] P. Pounds, A. Dollar, Hovering Stability of Helicopters with Elastic Constraints, Proceedings of the 2010 ASME Dynamic Systems and Control Conference, 2010.

[8] D. Mellinger, M. Shomin, N. Michael, and V. Kumar, Cooperative Grasping and Transport using Multiple Quadrotors, in Distributed Autonomous Robotic Systems, Lausanne, Switzerland, Nov 2010.

[9] N. Kuntz, P. Y. Oh, Towards Autonomous Cargo Deployment and Retrieval by an Unmanned Aerial Vehicle Using Visual Servoing,, in 2008 ASME Dynamic Systems and Controls Conference.

[10] http://dasl.mem.drexel.edu/pire/

[11] P. Corke, A robotics toolbox for MATLAB, IEEE Robotics and Automation Magazine, vol.3, pp.2432, Sept. 1996.

[12] L. Marques, J. Dinis, A. P. Coimbra, M. M. Crisstomo, J. P. Ferreira, "3D Hyper-Redundant Robot," in 11th Spanish Portuguese Conference on Electrical Engineering, Zaragoza, Spain, July 2009.

[13] N. Hogan, "Impedance control: an approach to manipulation," in American Control Conf, 1984.

[14] C. Korpela, T. Danko and P. Oh, "MM-UAV: Mobile manipulating unmanned aerial vehicle," Journal of Intelligent and Robotic Systems, vol. 65, no. 1-4, pp. 93-101, 2012.